

On the dynamic fracture of structural metals

ARES J. ROSAKIS and ALAN T. ZEHNDER

Graduate Aeronautical Laboratories, California Institute of Technology, Pasadena, CA 91125, USA

(Received September 1, 1984)

Abstract

Some fundamental aspects of dynamic crack growth in structural steels are presented and discussed. The discussion takes the form of a direct comparison of experimental results to elastic-plastic analyses, and attempts to clarify the role of material inertia and plasticity in the dynamic crack growth process. In addition the relation of crack growth criteria to micromechanical void growth models is considered.

Potential problems in the analysis of data obtained by either direct optical measurements or numerical simulations of crack growth are presented. It is demonstrated that large errors in the velocity records caused by stress wave effects are a main source of uncertainty in the interpretation of experimental results.

1. Introduction

For dynamic crack propagation under conditions of small scale yielding, fracture criteria based on the stress intensity factor are expressed in an analogous way to the static situation. This is done by the introduction of the quantity $K_I^d(t)$, which is the time dependent amplitude of the dynamic near tip asymptotic stress field [1], and a critical value K_{Ic}^d which is usually assumed to be a material property. Since the quantity K_{Ic}^d represents the resistance of the material to dynamic crack growth, its magnitude can be expected to depend on crack tip velocity as well as on the flow properties of the material. Thus for a propagating crack the fracture criterion is assumed to take the form:

$$K_I^d[a(t), t, \text{Load}] = K_{Ic}^d(\dot{a}), \quad (1.1)$$

where a , and \dot{a} are the crack tip position and velocity, respectively. The hypothesis expressed by (1.1) states that if the stress-intensity factor, evaluated by a purely elastodynamic analysis, is set equal to the material property function K_{Ic}^d , the dynamic fracture toughness, then the resulting equation of motion will determine $a(t)$ uniquely. The simplicity of the above hypothesis stems from the fact that all nonlinear and plasticity effects are lumped into the material property K_{Ic}^d . This quantity reflects the influence of material inertia on near crack tip nonlinearities and can either be measured by experiments or can be calculated on the basis of nonlinear models of crack growth and more basic, local, crack propagation criteria [2,3]. The question is therefore reduced to whether the fracture toughness K_{Ic}^d can be safely considered a unique function of crack tip velocity and material properties. The answer, which is still the subject of considerable discussion, seems to depend strongly on the material considered.

2. Limitations of near tip asymptotic solutions

The analytical difficulties associated with the dynamic crack propagation problem in both elastic and elastic-plastic solids have limited the number of available dynamic solutions to

idealized situations. In elastic solids, the existing analytical results are valid only until stress waves, reflected from the boundaries, reach the moving crack tip [1]. In ductile materials, there seem to be unresolved differences in the few available asymptotic solutions. In particular, for dynamic plane-strain crack growth in elastic-perfectly plastic materials obeying an associated flow rule, Slepyan [4], Achenbach and Dunayevsky [5] and more recently Gao and Nemat-Nasser [6], obtained three different dynamic asymptotic near-tip solutions. In all cases it was assumed that the yield condition was satisfied at all angles around the crack tip, thus excluding the possibility of a sector of elastic unloading. Achenbach and Dunayevsky used the Tresca yield criterion and concluded that for finite crack tip speeds the strains are bounded whereas a logarithmic singularity is recovered for $\dot{a} = 0$. Also, they showed that for zero crack tip speed and $\nu = 0.5$ the stress field reduces to the Prandtl field. On the other hand Gao and Nemat-Nasser, using the von Mises yield condition, concluded that the strain field varies logarithmically for non-zero crack tip speeds.

Recent finite element work of Lam and Freund [2] on the same problem indicates good agreement between the numerically predicted stress field and the results of Achenbach and Dunayevsky. The numerical work also strongly suggests the possibility of an elastic unloading sector behind the active plastic zone, a result that seems at variance with all available asymptotic analyses. The issue is complicated even further by clear indications that the range of applicability of the asymptotic results diminishes very rapidly and eventually disappears as the crack tip velocity vanishes. This has been clearly demonstrated for the case of mode-III elastic-plastic crack growth by Freund and Douglas [3]. By using a full field analytic solution they were able to demonstrate that the equivalent dynamic asymptotic result due to Slepyan [4] has a validity range of less than a hundredth of the plastic zone (process-zone size) for crack tip velocities less than $0.3 C_s$. This limitation which is also expected to apply, at least qualitatively, to the mode-I asymptotic dynamic solutions presents a major drawback in the applicability of the analytical results. Such uncertainties and limitations make numerical methods and direct experimental observations necessary for the complete understanding of the dynamic fracture event.

3. The effect of inertia on dynamic fracture toughness

3.1. Analytical and numerical predictions

For crack propagation in elastic-plastic solids under conditions of contained yielding, (most structural steels) some theoretical speculations can be made about the nature of the dependence of the dynamic fracture toughness on crack tip speed. It can be argued from a purely intuitive point of view that in the fracture of rate independent elastic-plastic materials the plastic zone surrounding the tip will give rise to greater inertia forces as the velocity of crack propagation increases and also that the effect will be much larger than in purely elastic materials. Approaching the problem from both an analytical and numerical point of view, Freund and Douglas [3] and Douglas [7] were able to study the steady state motion of mode-III cracks, propagating dynamically in an elastic, perfectly-plastic solid. The material was characterized by the von Mises yield criterion and a J_2 flow theory of plasticity. The results were concerned both with the full deformation field, which was determined by means of the finite element method, and with the deformation on the crack line within the active plastic zone, which was determined analytically. Although the full field numerical analysis was conducted under the assumption of small scale yielding, the analytical result did not depend on this restriction. The main observation on the strain distribution was that the level of plastic strain is significantly reduced from its corresponding slow crack growth levels due to material inertia. If this result is combined with the

requirement of a fixed level of plastic strain at a critical distance in front of the crack tip (a criterion proposed by McClintock and Irwin [8]) it can be expected that, for crack growth to occur, the far field stress intensity factor would necessarily increase with increasing crack speed. To quantify this idea Freund and Douglas [3] related the remotely applied stress intensity factor to the plastic zone strain distribution through the full-field numerical solution. The result displayed here in Fig. 1, demonstrates the variation of K_{IIIc}^d with crack tip velocity. The parameters appearing in Fig. 1 are the elastic shear wave speed c_s , the critical plastic strain γ_f and the level of applied stress intensity K_{IIIc} required to satisfy the same fracture criterion for crack initiation in the same material.

With a similar view toward developing a theoretical relation between K_{Ic} and crack tip speed, Lam and Freund [2] have analyzed the elastic-plastic, mode-I problem. In their work the stress intensity factor was related to the near tip crack opening displacement through the full field numerical solution. A critical crack tip opening angle growth criterion was imposed which was similar to that used by Dean and Hutchinson [9] and by Lam and McMeeking [10]. As in the mode III problem, the approach was based on the requirement that the same growth criterion can be applied to both initiation and crack propagation in the same material. The results are presented here in Fig. 2. The figure

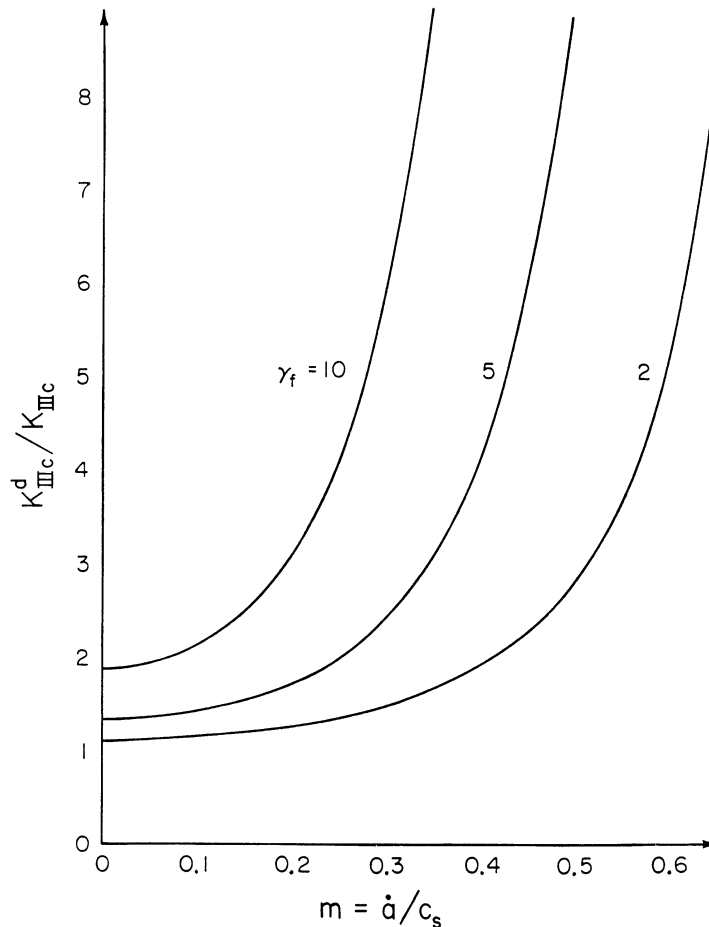


Figure 1. Mode III dynamic fracture toughness as a function of crack tip velocity in an elastic-ideally plastic rate insensitive material, according to the critical plastic strain fracture criterion. (From Freund and Douglas [3].)

shows the variation of K_{Ic}^d/K_{Ic} with normalized crack speed for different values of the ratio δ_c/r_m where δ_c is the critical value of the crack opening displacement at a characteristic distance r_m measured from the crack tip along the crack faces.

The importance of this result is amplified by the possibility of direct comparison with experiments performed in metals that fracture with a locally ductile mechanism while preserving the requirements of small scale yielding. Indeed, the numerical prediction corresponding to the value of $\delta_c/r_m = 32$ seems to agree well with the experimental data for dynamic crack growth in an AISI 4340 steel which was reported by Rosakis [11] and Rosakis, Duffy, and Freund [12,13] which data are also included in Fig. 2. The measurements were performed by means of the optical method of reflected caustics with a double cantilever beam specimen in a wedge loaded configuration. The data points represent the cumulative result for three identical specimens. As explained in detail in [2], knowledge of the material properties of this particular 4340 carbon steel (heated to 843°C, oil quenched and tempered at 316°C for an hour, $\sigma_0 = 1300$ MPa, $K_{Ic} = 30$ MPa \sqrt{m}) dictate the choice of $\delta_c/r_m = 32$ and allow the direct comparison of the experimentally obtained curve to this particular member of the K_{Ic}^d/K_{Ic} vs. \dot{a}/c_s family.

It should perhaps be noted at this point that the crack growth in the dynamic experiments was not steady state whereas the numerically obtained curves were derived using the steady state assumption. Thus direct comparison between the two results is possible only if the dynamic fracture toughness is a weak function of crack tip acceleration. Experiments reported recently by Brickstad [14] and described in detail in Section 3.2 (Fig. 3) indicate that this is indeed the case for some structural steels.

Local crack initiation and growth criteria such as the ones described above, represent attempts to model some of the basic features of the micromechanics of the fracture

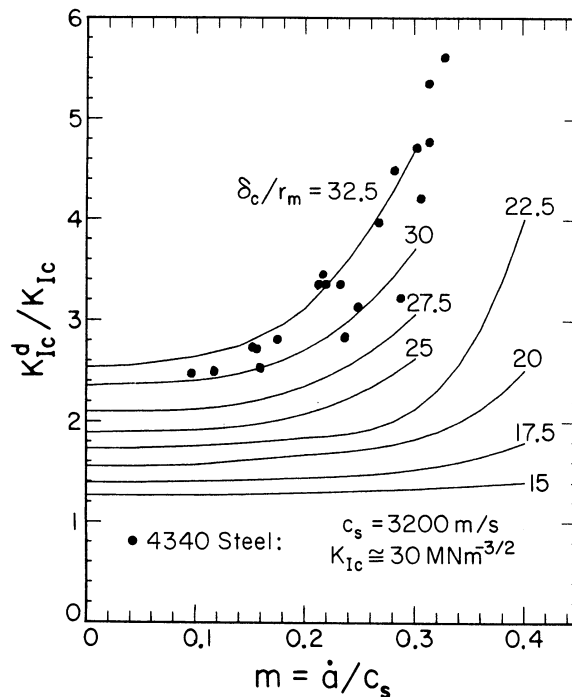


Figure 2. Mode-I dynamic fracture toughness as a function of velocity according to the critical crack tip opening angle fracture criterion. Also included are experimental results of Rosakis, Freund and Duffy [13] for 4340 steel. (From Lam and Freund [2].)

process. The fracture of ductile metals has been observed to occur by the initiation, growth, and coalescence of voids (Beachem [15] and Rosenfield [16]). Such voids are generated by plastic flow in a zone of intense straining surrounding the crack tip, called the process zone. Requiring that a certain displacement or strain reaches a critical value at a characteristic distance away from the tip is equivalent to identifying this characteristic size with the process zone. Inside this zone, the continuum theory is no longer strictly applicable. Thus, the development of comprehensive fracture criteria requires a detailed study of void growth under the macroscopically imposed crack tip field. The mechanism of quasistatic plastic hole growth was initially studied by McClintock [17] and by Rice and Tracey [18]. Both investigations emphasized the important role of triaxial stress states in enhancing void growth in the near-tip region. As pointed out by Rice [19], the high near-tip triaxiality can nucleate voids from preexisting inclusions or impurity particles and can lead to a macroscopically brittle crack behavior in metals which on the microscale are significantly ductile. An example of such behavior can be observed in the particular heat treatment of the AISI 4340 steel tested in [13].

For dynamic crack growth in metals which fracture by the locally ductile mechanism of hole growth under small scale yielding conditions, as in the cases described above, quantitative estimates of the influence of material ductility and inertia on the relationship between K_{IC}^d and \dot{a} can be made. Glennie [20] modified the void growth formulation of Rice and Tracey to include the effect of inertia, and obtained an approximate solution by means of a variational method. More recently Rosakis, Duffy, and Freund [13], following a similar approach, used an elementary argument to estimate the relative influence of inertia in the near tip ductile hole growth process. They showed that the total energy required for dynamic hole growth in front of a propagating crack tip, (kinetic energy plus dissipation through plastic work), normalized by the plastic work, is an increasing function of crack tip speed. The sensitivity of this ratio to crack tip speed was found to depend on the flow stress of the material. It was demonstrated that for more ductile solids,

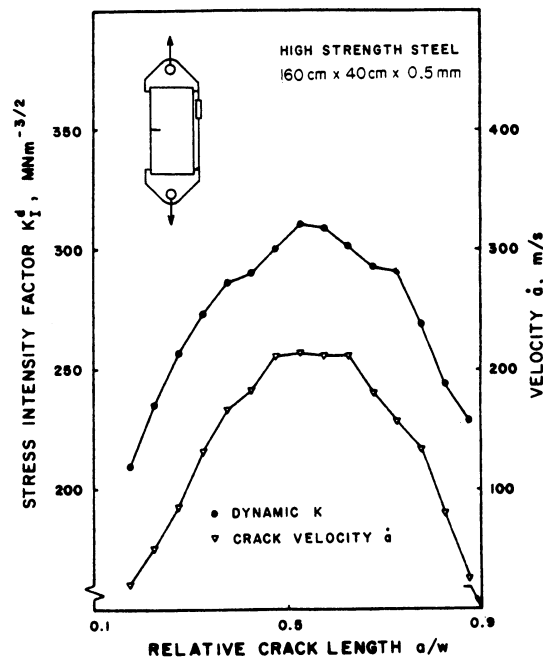


Figure 3. Stress intensity factor and crack velocity as functions of crack length. (From Brickstad [14].)

the inertia effects become important at lower speeds than in brittle solids, a behavior consistent with the results displayed in Fig. 2.

3.2. Experimental predictions

The available experimental results in the dynamic fracture of metals are limited to crack propagation under small scale yielding conditions. The principal purpose of such investigations is to observe the instantaneous stress intensity factor, and to determine whether or not the observed variation constitutes a material characteristic. The experiments can be divided into boundary value and direct measurements.

Boundary value measurements

The boundary value techniques involve measurement of crack tip position vs. time and either measurement of the time-dependent load applied to the specimen (Birkstad [14], Kanazawa et al. [22]) or an assumption regarding the nature of the boundary conditions (Bilek [23]), i.e. fixed displacement or constant rate of displacement at the load points. The results of such measurements are used in conjunction with a dynamic numerical model for the prediction of the stress intensity factor history.

Along these lines, Birkstad tested SEN steel specimens loaded in tension. The time dependent boundary conditions were measured with strain gages and the crack tip speed was recorded by using the R.F. current technique developed by Carlsson [24], to obtain a continuous recording of crack length. The energy release rate, and hence K_I^d , was then obtained by calculating the work done by the closing forces at the crack tip by means of a dynamic FEM program. By using a stretching screw on the side of the specimen away from the machined precrack, an initially increasing and subsequently decreasing K field was obtained. This produced both acceleration and deceleration phases of crack growth and allowed the study of the sensitivity of the dependence of the fracture toughness on \dot{a} . Results from a single specimen are presented in Fig. 3 where both K_I^d and \dot{a} are given as a

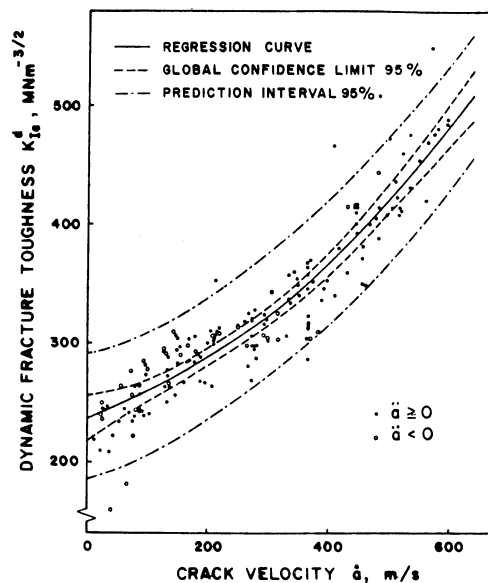


Figure 4. Dynamic fracture toughness as a function of crack velocity for a high strength steel. (From Birkstad [14].)

function of crack length. As is obvious from this figure, the crack tip velocity and K_I^d vary in phase both in the acceleration and deceleration regimes of the crack growth history, clearly indicating a relation between the two quantities. To demonstrate this more clearly, the collective data from many specimens is presented in Fig. 4 where a clear relation between K_{Ic}^d and \dot{a} is indicated while no dependence on acceleration is observed, contrary to previously reported work [25].

Behavior very similar to the above was also reported by Bilek [23] who performed tests with DCB specimens of 4340 steel. In this work the crack tip speed was measured by the same R.F. current technique used in [14] and also by crack propagation (ladder) gages with a spacing of 0.2 cm. A dynamic, Timoshenko beam model of the DCB specimen was then used to infer the dynamic stress intensity factor history. Despite the large scatter due to the many different tests being presented, the variation of K_I with crack tip speed, illustrated here in Fig. 5 follows the same trend as in [13] and [14] and compares well with the superimposed results of Hahn et al. [27] and Angelino [28]. Angelino devised a unique procedure for the determination of K_I^d and the crack tip speed. Using small, three point bend specimens, a crack was propagated unstably for small distances. The material used was a carbon steel very similar to 4340. By measuring the crack length and time of propagation (about 7 μ s) the average velocity was obtained. Measurement of the strain energy in the specimen before and after crack propagation gave the fracture energy, which when divided by the fracture surface area yielded the energy release rate.

Additional confidence in the existence of a unique K_{Ic}^d vs. \dot{a} relation in steel is obtained by Kanazawa et al. [22]. They performed experiments using both DCB and large SEN specimens subjected to uniform tension. The crack tip position was recorded by the use of gages spaced 3 cm apart. This information produced an *average* velocity record that was used in conjunction to a dynamic finite different code. By computing the energy variation, the dynamic energy release rate was obtained by a global energy balance in the specimen. Of particular interest are results corresponding to SEN specimens tested with a linear temperature gradient varying from -100°C on one side to $+50^\circ\text{C}$ on the other, the temperature increasing with crack length. As the crack propagated into the higher temperature region it decelerated and eventually stopped. The family of K_{Ic} vs. \dot{a}

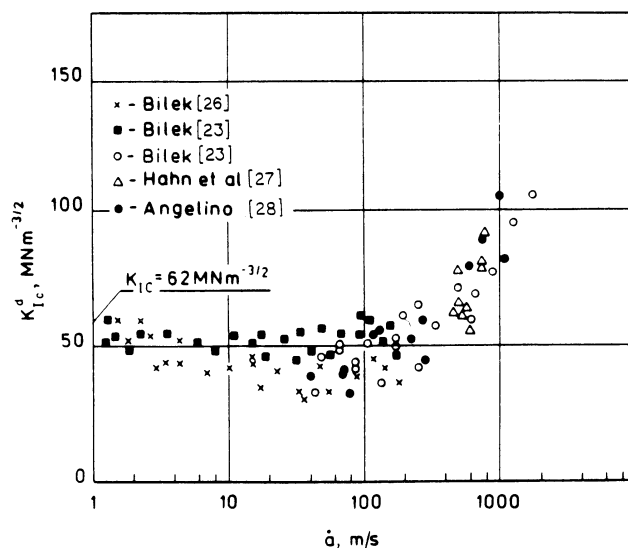


Figure 5. Dynamic fracture toughness as a function of crack velocity for 4340 steel. (From Bilek [23].)

relations presented in Fig. 6, corresponding to different temperatures, can explain the observed deceleration behavior of the cracks. The fracture toughness $K_{Ic}^d(\dot{a})$ increases with temperature (and hence crack length in these tests), however the stress intensity factor K_{Ic}^d available was nearly constant, thus to satisfy (1.1) the crack must slow down until $K_{Ic}^d(\dot{a}) = K_I^d$. Cumulative results for -40°C are given in Fig. 7. It has been theorized [29] that the vertical bands of constant speed shown in the high velocity region of this curve are due to non-uniqueness in the K_{Ic}^d vs. \dot{a} relation, and is similar to the behavior observed in Homalite-100 [30]. The authors would like to point out that in the above tests the wide gage spacing (3 cm) only gives an averaged record of crack tip speed. Thus an alternative explanation is that fine variations in the velocity are not detectable, leading to different values of K_I^d being assigned to the same average velocity (vertical lines).

Direct optical measurements

For the investigation of crack growth in transparent materials the techniques of photoelasticity and transmitted caustics have been used extensively in conjunction with high speed photography. Through application of these techniques, important advances in the study of rapid fracture have been achieved particularly by Dally [31], by A.S. Kobayashi [32,33] by Kalthoff and coworkers [34] and by Ravi-Chandar and Knauss [21]. These methods have been extended to metals through the use of photoelastic coatings and reflected caustics. Other techniques such as dynamic interferometry, moiré and the newly reported stress intensity factor tracer technique, are currently being explored [35,36]. As expected, the number of direct measurements performed on metallic fracture specimens is small compared to ones in clear polymers or glasses. This is due to the added technical difficulties introduced by reflected high speed photography and to the high level of effort associated with specimen preparation.

Birefringent coatings were first used in the study of the dynamic fracture of steel by T. Kobayashi and Dally [37]. As discussed in their work, the use of a single coating covering the surface of the metal specimen raises questions concerning the relative position of the crack tip, in the plastic coating and in the metal specimen. However, T. Kobayashi and Dally overcame this problem by cementing a pair of coatings to the surface of the grooved

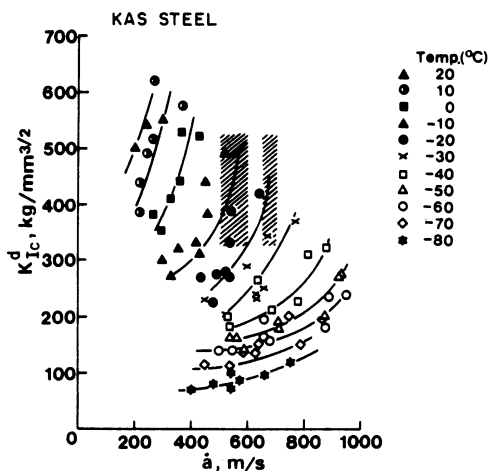


Figure 6. Dynamic fracture toughness as a function of crack velocity for different temperatures. $100 \text{ kg mm}^{-3/2} = 31 \text{ MNm}^{-3/2}$. (From Kanazawa et al. [22].)

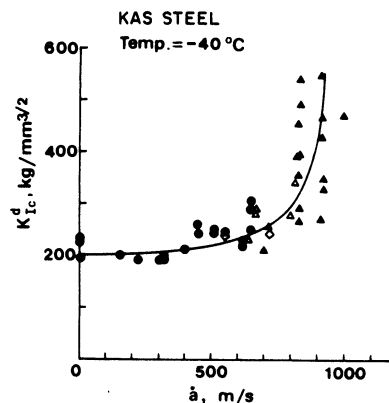


Figure 7. Dynamic fracture toughness as a function of crack velocity at -40°C . (From Kanazawa et al. [22].)

4340 steel specimen, one on either side of the groove. As the crack advanced they recorded the isochromatic patterns using a Cordin high-speed framing camera, from which they calculated the stress intensity as a function of time. They were also able to determine crack length and hence the crack velocity at each position. The results indicate large oscillations in the value of K_I^d corresponding to abrupt changes in the crack tip velocity. As discussed in detail in [12], the oscillations in K_I^d and in crack speed are in phase and are caused by the interaction of reflected stress waves with the propagating crack tip. Results from three different specimens are presented in Fig. 8 where the variation of K_{Ic}^d with \dot{a} is illustrated. The results follow the same qualitative trend as those reported by Bilek for a similar heat treatment of the 4340 steel. The specimen labeled 375 gave anomalous results, which were attributed by the authors to a different heat treatment.

The method of caustics (shadow spot method) for transparent materials was introduced by Manogg [38]. Through such contributions as those of Theocaris and Gdoutos [39], and Beinert and Kalthoff [34] this method has become established as a standard procedure for the measurement of the static and dynamic fracture toughness of nominally elastic, transparent materials. In addition, within the past few years, Rosakis [40] and Rosakis and Freund [41] provided analyses to account for the effects of material inertia and crack tip plasticity in the interpretation of caustic data obtained with light reflected from specimens of opaque structural materials. Extensive reviews of the method are given by Beinert and Kalthoff [34] and more recently by Rosakis and Zehnder [42] who presented the exact equations of caustics and discussed the consequences of mathematical approximations made by previous analyses.

The method was first applied to the study of the arrest process in high-strength steels, by Beinert and Kalthoff [34], but a relation between K_{Ic}^d and \dot{a} was not reported. More recently Rosakis [11], and Rosakis, Duffy, and Freund [12,13] used reflected caustics to study the dynamic behavior of cracks propagating rapidly in double cantilever beam specimens of 4340 steel. The caustic patterns formed during the course of the experiments were recorded by means of a high speed camera of the Craz-Schardin type. The instantaneous value of the dynamic stress intensity factor and the crack tip position were thus recorded. The results of the experiments indicate that the dynamic fracture toughness is an increasing function of crack tip speed (see Fig. 2). These values exceed those of

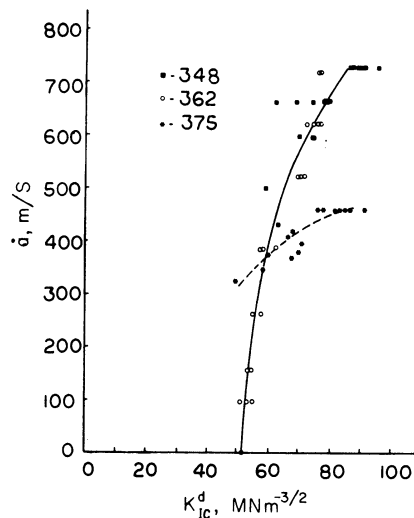


Figure 8. Dynamic fracture toughness as a function of crack velocity for a 4340 steel. (From Kobayashi and Dally [37].)

T. Kobayashi and Dally and those of Bilek et al. by a consistent 10%. This difference can easily be attributed to different mechanical properties due to differences in heat treatment. Of greater significance than the absolute values of K_{Ic}^d is the general shape of the curve and the qualitative agreement with the numerical results of Lam and Freund as demonstrated in Fig. 2.

A second feature of these results that is consistent with the observations of T. Kobayashi and Dally are the oscillations in the time records of K_{Ic}^d and \dot{a} . These oscillations were also correlated with the arrival time of stress waves that were initially emitted from the accelerating crack tip and subsequently reflected from the DCB specimen boundaries. Recent results obtained by Rosakis and Zehnder [43], presented here in Figs. 9 and 13a, also display such oscillations. Shown in Fig. 13a are the arrival times of waves reflected from the lateral sides, loading pins and the end of the cantilever arms of the DCB specimen. A detailed discussion on the influence of the reflected waves on dynamic crack advance can be found in [12 and 13]. Visual evidence of the existence of unloading waves generated at the propagating crack tip are shown in Fig. 10a. The photograph was taken by the present authors with the experimental setup sketched in Fig. 11. The photograph shows the caustic image of a dynamic crack ($\dot{a} = 1000$ m/s) and also the shadow images of unloading waves generated at the tip. The waves were found to propagate with the Rayleigh wave speed. It is perhaps worth noting here that only waves that produce out of plane displacements on the polished specimen surface can be detected by the caustics setup. Under idealized plane stress conditions this limits the possibilities to either Rayleigh waves propagating on the plate surface, or dilatational waves which produce a lateral contraction of the planar specimen due to the Poisson ratio effect.

Plane stress has been a key assumption in the interpretation of results from caustics

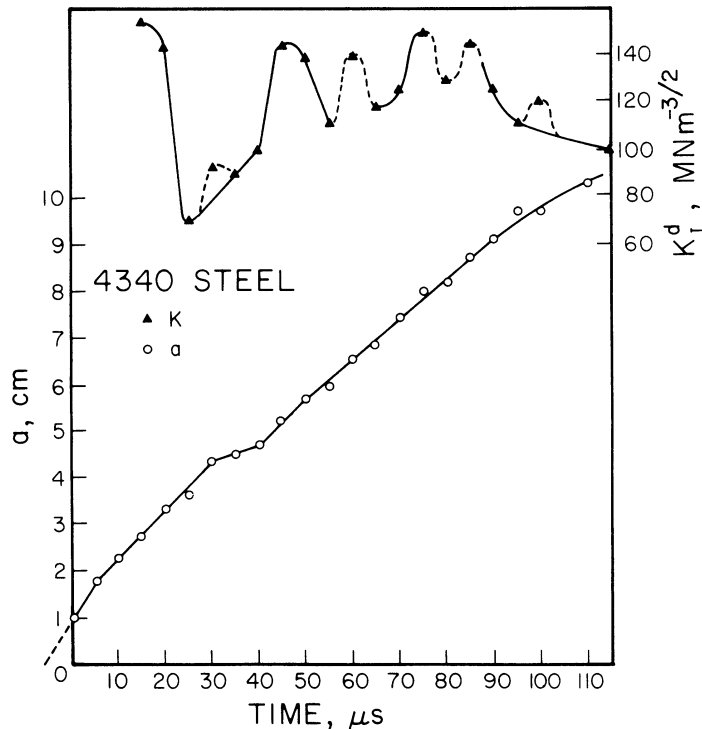


Figure 9. Stress intensity factor and crack length as a function of time for a DCB specimen of 4340 steel. (Rosakis and Zehnder, work in progress, Caltech 1984.)

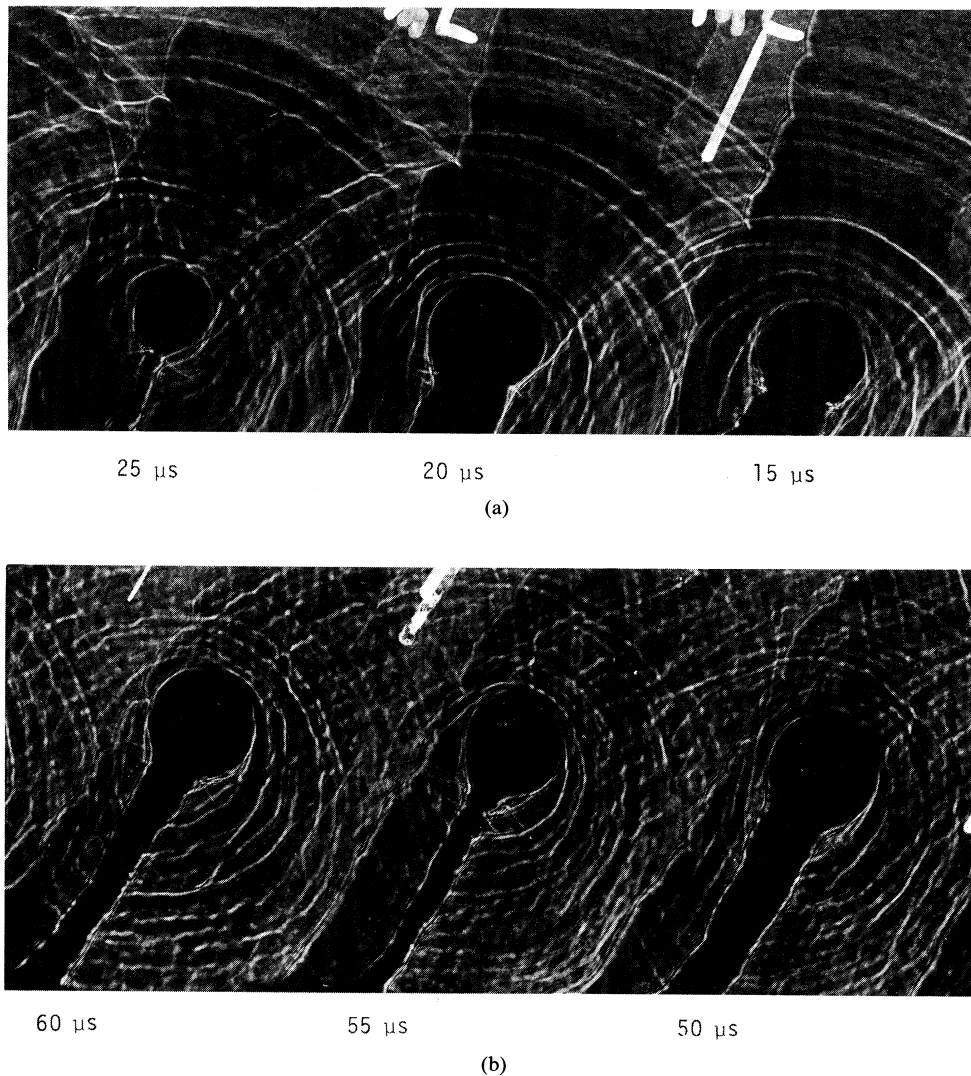


Figure 10. Reflected caustic patterns corresponding to dynamic crack growth test recorded in Fig. 9 for 4340 steel. (a) Strong dynamic effects are demonstrated by visible unloading waves and oscillations in caustic diameter. (b) Visible oscillations in the width of wake indicate vibrations of the cantilever arms of DCB specimens. (Rosakis and Zehnder, work in progress, Caltech 1984.)

data. In particular it has been assumed that at distances sufficiently far from the crack tip, the stress and displacement fields are adequately described by the theory of plane stress elasticity. Under the action of the applied loads, the specimen undergoes nonuniform out-of-plane deformation (thinning) whose intensity is completely characterized by the elastic plane-stress intensity factor.

With a view towards establishing the limitation of the plane stress interpretation of caustics data, Rosakis and Ravi-Chandar [44] tested compact tension specimens with sharp, planar straight-fronted cracks. The specimens were loaded to a fixed level and then shadow spot data were taken at different distances from the crack tip. This was achieved by adjusting the optical arrangement used in the experiment. Some of their results are

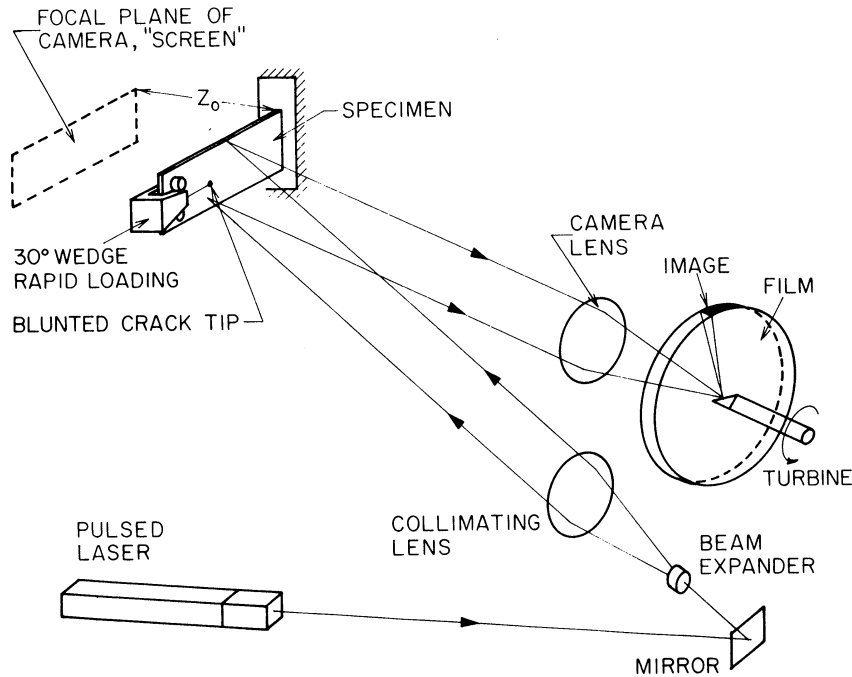


Figure 11. Experimental set-up for reflected, high speed photography of caustics. (Rosakis and Zehnder, work in progress, Caltech 1984.)

shown in Fig. 12. The figure contains data for martensitic 4340 steel specimens of several thicknesses. The ordinate is the ratio of the optically determined stress intensity factor (at different measurement distances from the crack tip) to the corresponding plane stress value obtained by boundary value measurements. The abscissa is the distance r from the crack tip (where the measurement was performed) normalized by the specimen thickness h . The results indicate that plane-stress conditions prevail at distances from the crack tip greater than half the specimen thickness. This conclusion is consistent with the crack tip

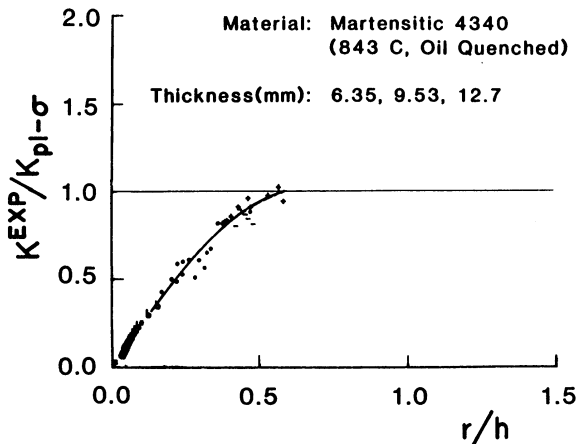


Figure 12. Static stress intensity factor as determined by caustics, divided by plane stress value for different distances, r , from the crack tip. (From Rosakis and Ravi-Chandar [44].)

boundary layer solution of Yang and Freund [45] and with the numerical results of Levy, Marcal, and Rice [46]. No such analysis exists for the dynamic problem. Nevertheless, using the static case as a guideline, the present authors feel that accurate optical measurements based on two-dimensional theory (photoelasticity, interferometry, caustics) can be performed with confidence only at distances greater than one half the specimen thickness.

Plasticity at the crack tip also limits the minimum distance from the tip where optical measurements can be performed. Analysis by Rosakis and Freund [41] has shown that the error introduced through the neglect of plasticity effects in the interpretation of caustics data will be small as long as the measurement is performed in a radius greater than twice the plastic zone size. Also, for any extent of the plastic zone, inertia effects appear to be significant for crack speeds exceeding approximately $0.2 c_1$, where c_1 is the longitudinal wave speed. Analysis of caustics formed by reflection of light from within the plastic zone exists only for stationary cracks [47].

4. Techniques of velocity measurement and inaccuracies due to errors in the velocity records

Accurate measurement of instantaneous crack tip speed is both very difficult and very important. The large scatter seen in K_{IC}^d vs. \dot{a} data such as Figs. 5 and 7 is most likely due to inaccurate crack tip position records resulting in poor velocity calculations. Several techniques, which can be divided into continuous and discrete are mentioned here and discussed. For a more thorough review see Weimer and Rogers [48].

One of the more widely used continuous measurements is the radio frequency skin effect technique developed by Carlsson [24]. High frequency currents tend to travel on the surface of a conductor, a behavior commonly referred to as the skin effect. By positioning terminals on either face of the crack, the path traveled by the current and thus the effective impedance increases linearly with crack length. Recording the impedance then gives a continuous record of the crack length history. An alternative method based on the overall change in the resistance of a metal specimen, due to crack growth, was developed by Congleton and Denton [49]. It was found that the change in potential of a direct current passed from one side of a steel SEN specimen to the other can be used to obtain a continuous record of crack tip position.

Discrete measurements involve either high-speed photography, as in photoelasticity and caustics, or a grid of conductive material of some type placed on the specimen along the prospective crack path [23,49,50]. As the crack runs, the conducting strips are broken and the resistance of the whole grid is increased. This stepwise change in resistance can be observed by using a bridge circuit and a recording oscilloscope. The crack length $a(t)$ is then known and can be differentiated to yield the crack tip velocity. Similarly, measurements of crack length at fixed time intervals are taken with high speed photography.

If the interval of measurement is not small enough, large errors may result due to variations in velocity on time scales smaller than the time interval. This can be expected to cause problems in small specimens where reflections of stress waves from the boundaries may cause abrupt changes in crack tip position. The $a(t)$ record is then subject to interpretation. For example, consider the $a(t)$ records in Fig. 13 obtained with the aid of caustics in experiments performed by the authors on 4340 steel. For this record data were obtained at intervals of $7 \mu\text{s}$. In Fig. 13b a smooth curve is drawn through the points producing one $\dot{a}(t)$ record. In Fig. 13a kinks are allowed in the $a(t)$ record at points where the first reflected stress waves arrive at the crack tip. This is done by fitting smooth curves to the right and left of the wave arrival time and then matching the curves at the wave arrival, allowing a discontinuity in slope. As can be seen the second interpretation produces a much different $\dot{a}(t)$ record. As a result of the above, the authors feel that in

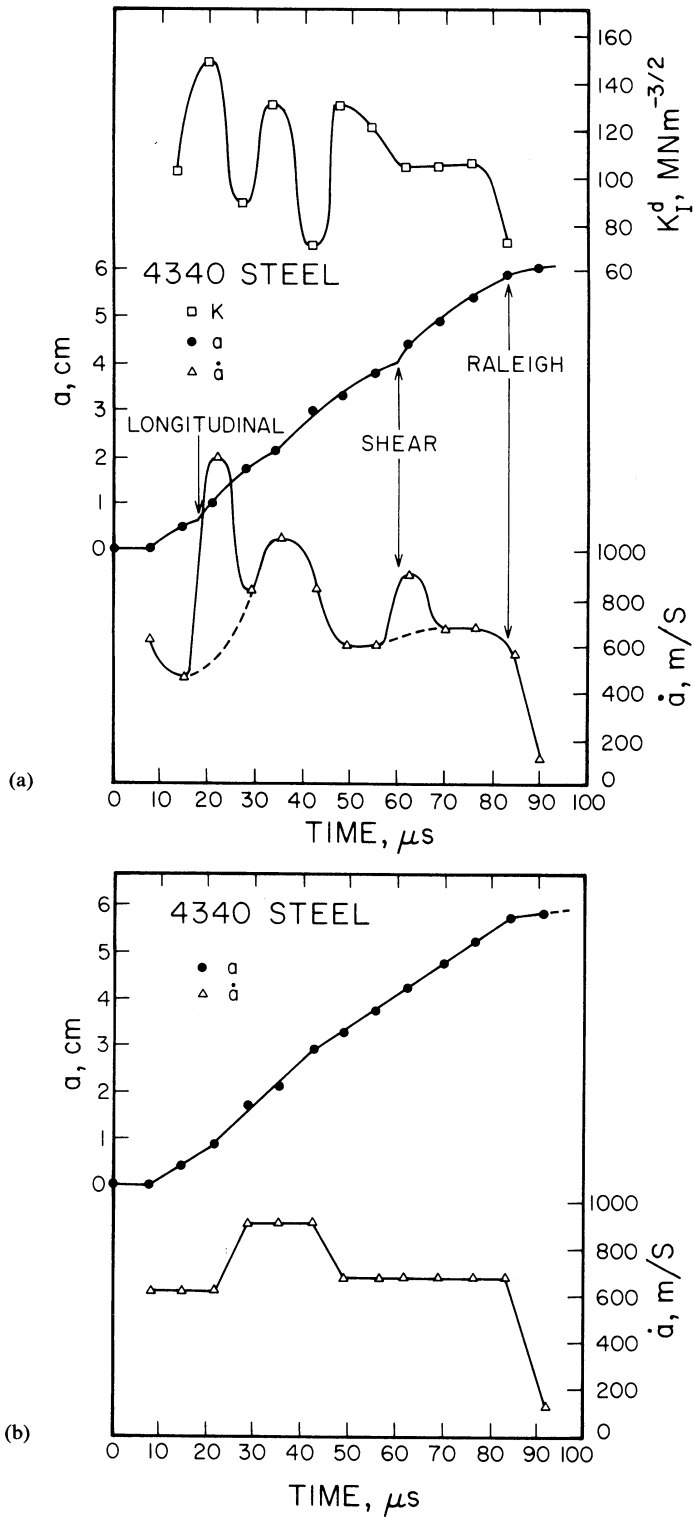


Figure 13. (a) Stress intensity factor, crack length and crack velocity as functions of time. Arrows indicate reflected stress wave arrivals. (b) Alternative interpretation of $a(t)$ record. (Rosakis and Zehnder, work in progress, Caltech 1984.)

order to achieve accuracy in $\dot{a}(t)$, the crack tip position must be measured at intervals less than $5\mu\text{s}$, preferably at least every $2\mu\text{s}$. This is particularly true for metals where the typical terminal velocities are three times higher than in polymers.

Some consequences of velocity record uncertainty were investigated by Hodulak, A.S. Kobayashi and Emery [51] who demonstrated the sensitivity of computed K_I^d values to crack velocities used as input to FEM programs. For wedge loaded RDCB specimens of Araldite B, they used the measured $a(t)$ record to compute $K_I^d(t)$. They then perturbed the experimental $a(t)$ and recalculated $K_I^d(t)$. Their results show that small errors in velocity can severely perturb the predicted value of K_I^d .

Further indications of this can be seen in the work of Nishioka and Atluri [52]. They performed a FEM simulation of Kalthoff's experiments in 9 mm thick wedge loaded RDCB specimens of high strength steel [53]. Kalthoff's $K_I^d(a)$ and $\dot{a}(a)$ records are given in Fig. 14 together with the numerically predicted values. Note that the calculated K_I^d does not show the oscillations that Kalthoff et al. report and attribute to wave interactions. A possible explanation of the discrepancy may lie in the fact that an averaged velocity record was used. In particular, for the first 200 mm, a straight line was drawn through the $a(t)$ data, resulting in constant velocity, whereas for longer crack lengths the velocity is not averaged. As evident from the figure, it is in this region ($a > 200$ mm) that the calculated K_I^d agrees with the measured values. The work of Hodulak et al., indicates the possibility that the disagreement between the measured and calculated K_I^d is due to not inputting accurate velocity measurements to the FEM analysis.

Further consequences of uncertainties in the velocity record, in the presence of stress wave reflections, are also demonstrated by Dahlberg, Nilsson and Brickstad's [54] results reproduced here in Figs. 15a, b. They used SEN specimens loaded in uniform tension. The results in Fig. 15a are for specimens 60 cm high, those in Fig. 15b are for specimens 160

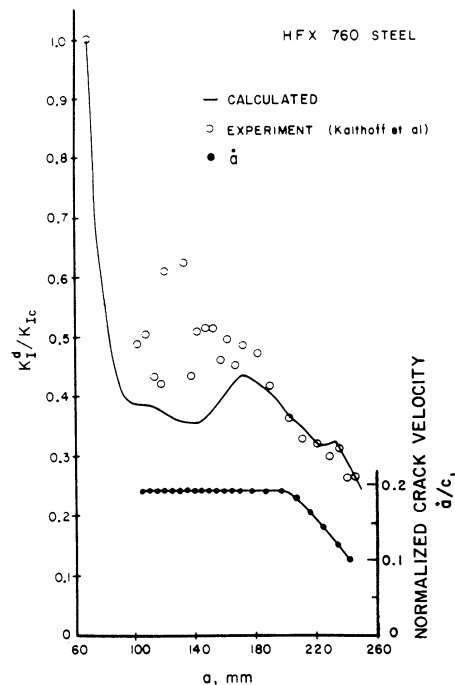


Figure 14. Experimentally determined crack velocity and stress intensity factor (from Kalthoff et al. [53]) and computed stress intensity factor (from Nishioka and Atluri [52]).

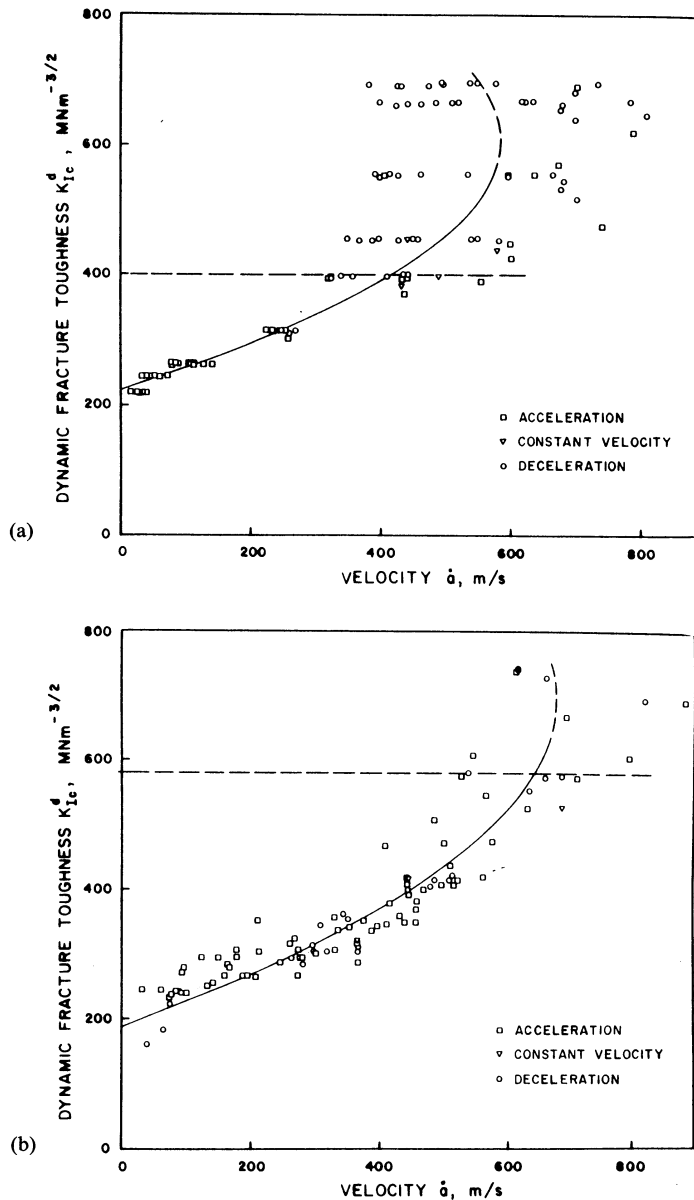


Figure 15. Dynamic fracture toughness as a function of crack velocity for SEN specimens of high strength steel. Specimen dimensions, (a) 60 cm \times 40 cm \times 0.5 mm (b) 160 cm \times 40 cm \times 0.5 mm. Increased scatter in smaller specimen. (From Dahlberg, Nilsson, and Brickstad [54].)

cm high. The crack velocity was measured using the impedance technique discussed earlier in this section which gives a continuous measure of $a(t)$. However, oscillations in $a(t)$ whether from electrical noise or stress waves, were smoothed out. In the smaller specimen where stress waves would be expected to cause variations in \dot{a} , there is much scatter in data. Note that for a given K_I^d level there is a range of velocities. This seems likely to be caused by experimental scatter in the velocities due to stress wave reflections. On the other hand, in the larger specimen, where reflected stress waves are *not* present, there is less scatter in the K_I vs \dot{a} data.

Evidence that stress waves do cause abrupt variations in K_I^d in DCB specimens is seen in Figs. 10a, b, photographs corresponding to the test recorded in Fig. 9. In Fig. 10a the width of the wake behind the caustic oscillates indicating oscillations in the beam arms of the DCB specimen. In Fig. 10b the caustic diameter is suddenly reduced from one frame to the next (5 μ s), due to the arrival of an unloading stress wave. This direct evidence of large oscillations in the DCB specimen cantilever arms clearly demonstrates that fixed grip conditions are not a good assumption for the numerical modelling of DCB specimens.

5. Concluding remarks

The qualitative agreement of results from three entirely different points of view (continuum models, experiment and microscopic void growth models) gives confidence in the use of the local, ductile, crack growth criteria discussed here. It also provides strong evidence for the existence of a unique dependence of K_{Ic}^d on crack tip speed in metals that fracture with a locally ductile mechanism of hole growth. For brittle solids the separation process seems to be stress controlled (generation of microcracks) and the above discussion is no longer applicable. This is demonstrated by the recent experimental results of Ravi-Chandar and Knauss [21] which indicate a non-unique K_{Ic}^d vs. \dot{a} variation in Homalite-100. However, no quantitative explanation, in terms of a microscopic fracture-process model, is yet available.

Acknowledgements

The authors would like to express their gratitude to Dr P.S. Lam and Professor L.B. Freund of Brown University for providing them with a copy of their work as well as with results displayed in Fig. 2, prior to publication of their work. The authors would also like to acknowledge the laboratory assistance of Mr. Sridhar Krishnaswamy. The research support of the National Science Foundation, Grant No. MEA-83-07785, as well as the support of an IBM (faculty development award) is also gratefully acknowledged.

References

- [1] L.B. Freund, in *Mechanics of Fracture*, ASME-AMD 19 (1976) 105–134.
- [2] P.S. Lam and L.B. Freund, *Journal of the Mechanics and Physics of Solids* (1984) to appear.
- [3] L.B. Freund and A.S. Douglas, *Journal of the Mechanics and Physics of Solids* 30 (1982) 59–74.
- [4] L.I. Slepyan, *Mekhanika Tverdogo Tela* (English translation) 11 (1976) 144–153.
- [5] J.D. Achenbach and V. Dunayevsky, *Journal of the Mechanics and Physics of Solids* 29 (1981) 283–303.
- [6] Y.C. Gao and S. Nemat-Nasser, *Mechanics of Materials* 2 (1983) 47–60.
- [7] A.S. Douglas, Ph.D. Thesis, Brown University (1981).
- [8] F.A. McClintock and G.R. Irwin, in *Fracture Toughness Testing and its Applications*, ASTM-STP 381 (1964) 95.
- [9] R. Dean and J.W. Hutchinson, in *Fracture Mechanics: Twelfth Conference*, ASTM-STP 700 (1980) 383–405.
- [10] P.S. Lam and R.M. McMeeking, *Journal of the Mechanics and Physics of Solids* (1984) 395–414.
- [11] A.J. Rosakis, Ph.D. Thesis, Brown University (1982).
- [12] A.J. Rosakis, J. Duffy and L.B. Freund, in *Workshop on Dynamic Fracture Proceedings*. Edited by W.G. Knauss, K. Ravi-Chandar and A.J. Rosakis, California Institute of Technology (1983) 100–118.
- [13] A.J. Rosakis, J. Duffy and L.B. Freund, *Journal of the Mechanics and Physics of Solids* 32 (1984) 443–460.
- [14] B. Brickstad, *International Journal of Fracture* 21 (1983) 177–194.
- [15] C.D. Beachem, *Transactions of the American Society of Metals* 56 (1963) 318.
- [16] A.R. Rosenfield, *Metallurgical Reviews* 13, review 121 (1968) 29–40 and *Metals and Materials* 2 (1968).
- [17] F.A. McClintock, *Journal of Applied Mechanics* 35 (1968) 363–371.
- [18] J.R. Rice and D.M. Tracey, *Journal of the Mechanics and Physics of Solids* 17 (1969) 201.
- [19] J.R. Rice, in *Mechanics of Fracture*, ASME-AMD 19 (1976) 23–53.
- [20] E.B. Glennie, *Journal of the Mechanics and Physics of Solids* 20 (1972) 415–429.

- [21] K. Ravi-Chandar and W.G. Knauss, *International Journal of Fracture* 25 (1984) 247–262; 26 (1984) 65–80, 141–154, 193–204.
- [22] T. Kanazawa, S. Machida, T. Teramoto and H. Yoshinari, *Experimental Mechanics* (1981) 78–88.
- [23] Z. Bilek, in *Crack Arrest Methodology and Applications*, ASTM-STP 711 (1980) 240–247.
- [24] A.J. Carlsson, *Transactions of the Royal Institute of Technology*, Stockholm, 189 (1962).
- [25] B. Brickstad and F. Nilsson, *International Journal of Fracture* 16 (1980) 71–84.
- [26] Z. Bilek, *Scripta Metallurgica* 12 (1978) 1101–1106.
- [27] G.T. Hahn et al., Report to the U.S. Nuclear Regulatory Commission, Battelle Columbus Laboratories (1974–1976).
- [28] G.C. Angelino, in *Fast Fracture and Crack Arrest*, ASTM-STP 627 (1978) 392–407.
- [29] W.G. Knauss, Proceedings of the 6th International Conference on Fracture, New Delhi, Dec. 4–10, 1984.
- [30] W.G. Knauss and K. Ravi-Chandar, *International Journal of Fracture* 27 (1985).
- [31] J.W. Dally, *Optical Methods in Mechanics of Solids*. Edited by A. Lagarde, Sijthoff and Noordhoff (1980) 692.
- [32] A.S. Kobayashi, *Experimental Mechanics* 10 (1970) 106.
- [33] A.S. Kobayashi, in *Fracture Mechanics*. Edited by N. Perrone et al. University Press, Charlottesville, Virginia (1978) 481–496.
- [34] J. Beinert and J.F. Kalthoff, in *Mechanics of Fracture*, Vol. VII. Edited by G. Sih, Sijthoff and Noordhoff (1981) 281–330.
- [35] W.G. Knauss, R. Pfaff and C. Schultheisz. Private Communication. Caltech (1984).
- [36] K.S. Kim, *Journal of Applied Mechanics* (1985) to appear.
- [37] T. Kobayashi and J.W. Dally, *Crack Arrest Methodology and Applications*, ASTM-STP 711 (1980) 189–210.
- [38] P. Manogg, Ph.D. Thesis, University of Freiburg (1964).
- [39] P.S. Theocaris and E.E. Gdoutos, *Journal of Applied Mechanics* 39 (1972) 91.
- [40] A.J. Rosakis, *Engineering Fracture Mechanics* 13 (1980) 331–347.
- [41] A.J. Rosakis and L.B. Freund, *Journal of Applied Mechanics* 48 (1981) 302–308.
- [42] A.J. Rosakis and A.T. Zehnder, *Journal of Elasticity* (1985) to appear.
- [43] A.J. Rosakis and A.T. Zehnder, work in progress. Caltech (1984).
- [44] A.J. Rosakis and K. Ravi-Chandar, GALCIT Report SM 84-2 (March 1984).
- [45] W. Yang and L.B. Freund, Brown University Report (1984).
- [46] N. Levy, P.V. Marcal and J.R. Rice, *Nuclear Engineering and Design* 17 (1971) 64–75.
- [47] A.J. Rosakis and L.B. Freund, *Journal of Engineering Materials and Technology* 104 (1982) 115–120.
- [48] R.J. Weimer and H.C. Rogers, *Fast Fracture and Crack Arrest*, ASTM-STP 627 (1977) 359–371.
- [49] J. Congleton and B.K. Denton, in *Fast Fracture and Crack Arrest*, ASTM-STP 627 (1977) 336–358.
- [50] A.S. Kobayashi et al., *Journal of Engineering Materials Technology* 100 (1978) 402–410.
- [51] L. Hodulak, A.S. Kobayashi and A.F. Emery, *Fracture Mechanics: Twelfth Conference*, ASTM-STP 700 (1980) 174–188.
- [52] T. Nishioka and S.N. Atluri, *Engineering Fracture Mechanics* 16 (1982) 157–175.
- [53] J.F. Kalthoff et al., in *Crack Arrest Methodology and Applications*, ASTM-STP 711 (1980) 109–127.
- [54] L. Dahlberg, F. Nilsson and B. Brickstad, in *Crack Arrest Methodology and Applications*, ASTM-STP 711 (1980) 89–108.

Résumé

On présente et on discute certains aspects fondamentaux de la croissance dynamique d'une fissure dans des aciers de construction. La discussion prend la forme d'une comparaison directe des résultats expérimentaux à l'analyse élasto-plastique et tente de clarifier le rôle de l'inertie et de la plasticité du matériau dans le processus de croissance dynamique d'une fissure. On considère en outre la relation qui les critères de la croissance d'une fissure aux modèles micro-mécaniques de croissance des lacunes.

On présente les problèmes potentiels que peuvent surgir dans l'analyse des données obtenues par des mesures directes optiques ou par des simulations numériques de la croissance d'une fissure. On démontre que des erreurs importantes dans les enregistrements de vitesse causées par des effets d'onde de contrainte sont la source principale d'incertitudes dans l'interprétation des résultats expérimentaux.